Chem

CellPress

Article

Quantum-tunneling-mediated synthesis of prebiotic chelation agents in interstellar analog ices

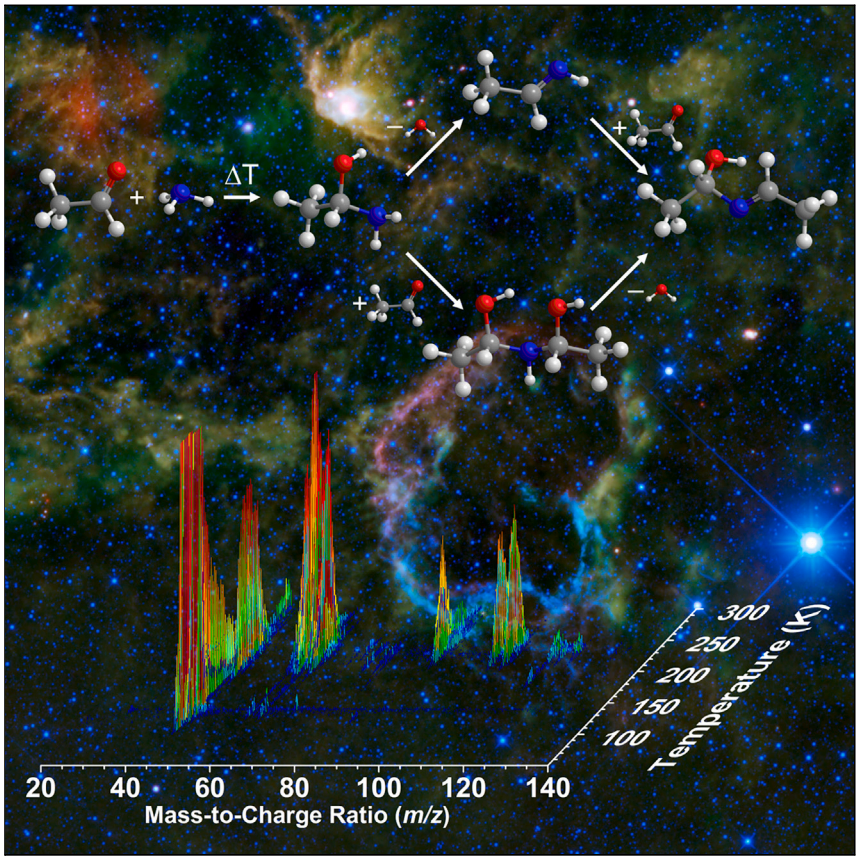

Ices in molecular clouds are usually expected to undergo reactions only when initiated by energetic cosmic radiation; however, ammonia (NH_3) and acetaldehyde (CH_3CHO) have been found to produce 1-aminoacetaldehyde ($CH_3C(OH)NH_2$) during heating, which simulates star formation. We demonstrate a complex set of reactions proceeding from 1-aminoacetaldehyde to ethanimine (CH_3CHNH), 1-ethylideneaminoethanol ($CH_3CH(OH)NCHCH_3$), and 1-(1-hydroxyethylamino) ethanol ($NH(CH(OH)CH_3)_2$), with the latter acting as a prebiotic chelating agent of main group I and II ions.

Joshua H. Marks, Anatoliy A. Nikolayev, Mikhail M. Evseev, ..., Ivan O. Antonov, Alexander M. Mebel, Ralf I. Kaiser

pfizeke@gmail.com (I.O.A.)
mebela@fiu.edu (A.M.M.)
ralfk@hawaii.edu (R.I.K.)

Highlights

Organic chelating agents are produced for the first time in interstellar ices

Ion chelation aids ion transport and membrane stability in primitive cells

Newly discovered molecules can promote RNA replication catalyzed by metal ions

Results guide radio astronomy searches for the origins of life in space

Marks et al., Chem 9, 1–18
November 9, 2023
https://doi.org/10.1016/j.chempr.2023.07.003

Please cite this article in press as: Marks et al., Quantum-tunneling-mediated synthesis of prebiotic chelation agents in interstellar analog ices, Chem (2023), https://doi.org/10.1016/j.chempr.2023.07.003

Chem

CellPress

Article

Quantum-tunneling-mediated synthesis of prebiotic chelation agents in interstellar analog ices

Joshua H. Marks,[1,2] Anatoliy A. Nikolayev,[3] Mikhail M. Evseev,[3] Jia Wang,[1,2] Andrew M. Turner,[1,2] N. Fabian Kleimeier,[1,2] Oleg V. Kuznetsov,[3] Mason McAnally,[1,2] Alexander N. Morozov,[4] Ivan O. Antonov,[3,*] Alexander M. Mebel,[4,*] and Ralf I. Kaiser[1,2,5,*]

SUMMARY

Ion transport is vital to all modern lifeforms, but how early cells could have accomplished this without complex proteins that are used by modern cells has remained elusive. Here, we demonstrate the rapid formation of prebiotic chelation agents through a complex set of reactions in interstellar analog ices of ammonia (NH_3) and acetaldehyde (CH_3CHO) using high-sensitivity and isomer-specific photoionization techniques. Driven by solvation, nucleophilic addition accesses 1-aminoethanol ($CH_3CH(OH)NH_2$) at temperatures as low as 65 K. The high sensitivity of photoionization mass spectrometry reveals an efficient preparation and the very first observation of 1-(1-hydroxyethylamino)ethanol ($NH(CH(OH)CH_3)_2$), a chelating agent, and 1-ethylideneaminoethanol ($CH_3CH(OH)NCHCH_3$). These findings expose facile, quantum-tunneling-mediated low-temperature routes to complex organics in cold interstellar environments and provide compelling abiotic pathways to prebiotic chelation agents of main group metals that enabled ion transport in primitive cells on early Earth.

INTRODUCTION

The "RNA world hypothesis" suggests that early lifeforms employed ribonucleic acid (RNA) as both genetic and functional material prior to the emergence of deoxyribonucleic acid (DNA) and proteins.[1–4] The molecular building blocks for such lifeforms (nucleotides,[5] amino acids,[6] and alkyl phosphates[7,8]) may have arisen abiotically through the chemical processing of ices in molecular clouds. In these interstellar environments, carbonaceous and silicate-based nanoparticles coated with a complex mixture of ices containing water (H_2O), methane (CH_4), ammonia (NH_3), carbon monoxide (CO), carbon dioxide (CO_2), and methanol (CH_3OH) support low-temperature thermal reactions and energetic non-equilibrium reactions initiated by galactic cosmic rays (GCRs) and vacuum ultraviolet (VUV) light.[9–11] Thermal reactions would have enabled an abiotic formation of RNA precursors in ices once a molecular cloud transitioned to star-forming regions and protostars formed. The protoplanetary disk about a protostar can easily reach average temperatures in excess of 200 K.[12] Under these conditions, complex molecules previously formed by energetic processing can undergo successive thermal reactions and yield more chemically complex and functionalized prebiotic molecules. Once the solar system was formed, the eventual delivery of these molecules via meteorites and comets to newly formed planets constituted a plausible source of prebiotic molecules on the early Earth.[13–15]

THE BIGGER PICTURE

The source of the chemical prerequisites for the origin of life is an enduring question that is foundational to astrochemistry and astrobiology. Early lifeforms must have had access to genetic and functional biomolecules, likely in the form of RNA and amino acids. Metal ions, such as magnesium, play a key role in stabilizing and replicating RNA. Contemporary cells use specialized proteins to transport ions through their membranes, which are too large and complex to have been available to primitive cells. Here, we present evidence of base-catalyzed nucleophilic addition and elimination reactions occurring at low temperatures accessible in the interstellar medium, leading to prebiotic chelating agents. Reactions of ammonia and acetaldehyde in model ice provide a compelling justification for the idea that reactions within ices can produce complex prebiotic molecules capable of chelating metal ions, facilitating ion transport into primitive cells, and ultimately catalyzing RNA replication.

Please cite this article in press as: Marks et al., Quantum-tunneling-mediated synthesis of prebiotic chelation agents in interstellar analog ices, Chem (2023), https://doi.org/10.1016/j.chempr.2023.07.003

In addition to these molecular building blocks, chemical pathways for RNA replication[16–18] and cell encapsulation by membranes[19–21] must have been readily available to primitive lifeforms. The universality of the phospholipid bilayer that comprises the selectively permeable plasma membrane of all contemporary cells points to its early development.[22] The hydrophobic interstitial layer of cell membranes poses a barrier to free diffusion of highly hydrophilic ions into the cell. Ion transport of sodium (Na^+), potassium (K^+), magnesium (Mg^{2+}), and calcium (Ca^{2+}) through the membrane is a vital process in biology as we know it.[17,18] Magnesium ions are of particular significance to the exploitation of RNA by early lifeforms because these ions have a catalytic effect on RNA replication, although they also exhibit a destabilizing effect on phospholipid membranes.[23,24] In modern cells, ion transport is mediated through complex transmembrane proteins, which either passively allow specific ions to pass through transmembrane channels or actively consume energy stored in adenosine triphosphate (ATP) to maintain nonequilibrium ion concentrations.[25,26] However, the chemical complexity of these transport proteins, which can frequently contain more than 15,000 atoms,[27] casts significant doubts on the possibility that primitive lifeforms could have employed them. Chelation of these ions by polydentate ligands, i.e., ligands that form multiple coordination bonds to the same ion, can be accomplished by much simpler molecules than proteins or polypeptides that should be more accessible to prebiotic chemistry and primitive biochemical pathways. Ion chelation can result in strong molecular affinity for ions, not because any of the bonds formed are particularly strong, but because of the contributions of many weaker bonds. The result is a reversible and non-covalent bond that can allow an ion to freely interact with its surroundings in a hydrophilic environment but can, given an appropriate structure, shield an ion from hydrophobic environments and permit its free diffusion. These polydentate ligands may have been present in the environment in which early lifeforms developed, during the time period before complex transmembrane proteins.[17,18] The nature of these polydentate ligands and their underlying formation pathways under prebiotic conditions has remained elusive; however, their presence was critical for efficient ion transport prior to the advent of advanced life on Earth.

Here, we present persuasive experimental and computational evidence of fundamental reaction mechanisms in low-temperature interstellar ices, which result in the formation of highly functionalized complex organic molecules (COMs)—organic molecules containing six or more atoms in the interstellar medium—capable of chelating metal ions in prebiotic environments. Exploiting interstellar model ices of ammonia (NH_3) with acetaldehyde (CH_3CHO), the exposed chemical network relies on nucleophilic addition and dehydration pathways[28] as vital components of the two-step nucleophilic substitution (S_N2) mechanism (Figure 1).[29] Although simple thermal reactions have been observed in interstellar ices,[30–43] the critical role of the primary products such as 1-aminoethanol (**1**, $CH_3CH(OH)NH_2$)[35] in the abiotic synthesis of prebiotic chelating agents has been elusive.[39] Here, products of the reaction of ammonia and acetaldehyde are expected to form in interstellar ices, where they can be preserved through low temperatures, about 10 K in a dense molecular cloud, or through sublimation and isolation in the gas phase at warmer temperatures up to 300 K once the cloud transitions into star-forming regions.[44,45] Considering the abundance of functional groups with non-bonding electrons on electronegative species, i.e., hydroxy (ROH) and amino (RNR′R″) moieties, the terminal products of the network (Figure 1) represent excellent primordial metal cation chelating ligands and would, in particular, promote the catalytic activity of magnesium ions (Mg^{2+}) toward RNA replication, while at the same time preserving cell membrane stability under prebiotic conditions.[16–18]

[1]W. M. Keck Research Laboratory in Astrochemistry, University of Hawai'i at Manoa, Honolulu, HI 96822, USA

[2]Department of Chemistry, University of Hawai'i at Manoa, Honolulu, HI 96822, USA

[3]Samara National Research University, Samara 443086, Russia

[4]Department of Chemistry and Biochemistry, Florida International University, Miami, FL 33199, USA

[5]Lead contact

*Correspondence: pfizeke@gmail.com (I.O.A.), mebela@fiu.edu (A.M.M.), ralfk@hawaii.edu (R.I.K.)

https://doi.org/10.1016/j.chempr.2023.07.003

Please cite this article in press as: Marks et al., Quantum-tunneling-mediated synthesis of prebiotic chelation agents in interstellar analog ices, Chem (2023), https://doi.org/10.1016/j.chempr.2023.07.003

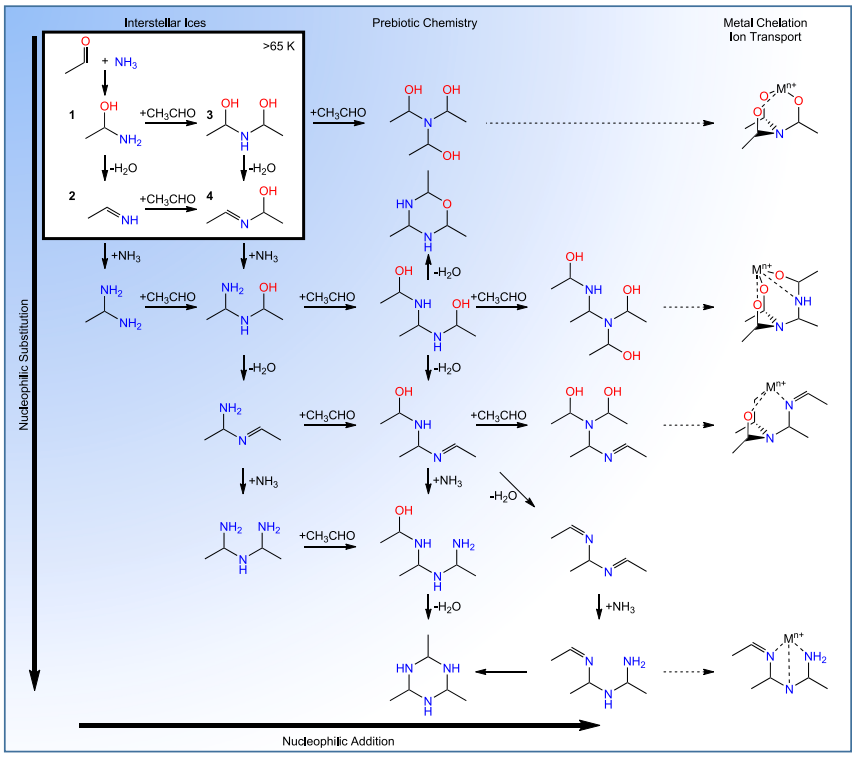

Figure 1. Reaction scheme for ammonia and acetaldehyde in interstellar ices

Observed species and reaction products thereof represent excellent metal chelating agents and may serve as prebiotic surrogates for ion transport proteins and enabling ion mobility in primitive cells.

Exploiting photoionization reflectron time-of-flight mass spectrometry (PI-ReToF-MS) in conjunction with Fourier transform infrared (FTIR) spectroscopy and electronic structure calculations, we report on a complex set of reactions that take place during the thermal processing of interstellar analog ices containing ammonia and acetaldehyde. These processes result in the formation of 1-aminoethanol (**1**, $CH_3CH(OH)NH_2$) and ethanimine (**2**, CH_3CHNH) along with the very first laboratory observations of 1-(1-hydroxyethylamino) ethanol (**3**, $NH(CH(OH)\ CH_3)_2$) and 1-ethylideneaminoethanol (**4**, $CH_3CH(OH)NCHCH_3$) (Figure 2). A reduction in the rate of low-temperature reaction is observed upon deuteration. This demonstrates a strong kinetic isotope effect[46] and suggests that *quantum tunneling* may affect reaction rates at temperatures relevant to astrophysical environments even for molecules as complex as **1**–**4**. *Nucleophilic addition* is demonstrated through the formation of **1** and **3**, and their *dehydration* yields **2** and **4**, respectively, in interstellar analog ice. These findings reveal a complex set of quantum-tunneling-mediated reactions that yield prebiotic chelating agents, fundamentally enhancing our knowledge of the achievable level of molecular complexity of organic molecules in deep space. The presence of these molecules enables facile RNA replication, once introduced through meteorites and comets onto early Earth, and provides the chemical prerequisites for the origins of life.

RESULTS AND DISCUSSION

Ice preparation

Cold, dense molecular clouds are composed of interstellar dust in the form of carbonaceous[47] and olivine-type siliceous[48] nanoparticles that accrete layers of ices composed largely of water (H_2O), methanol (CH_3OH), carbon dioxide (CO_2), and

Please cite this article in press as: Marks et al., Quantum-tunneling-mediated synthesis of prebiotic chelation agents in interstellar analog ices, Chem (2023), https://doi.org/10.1016/j.chempr.2023.07.003

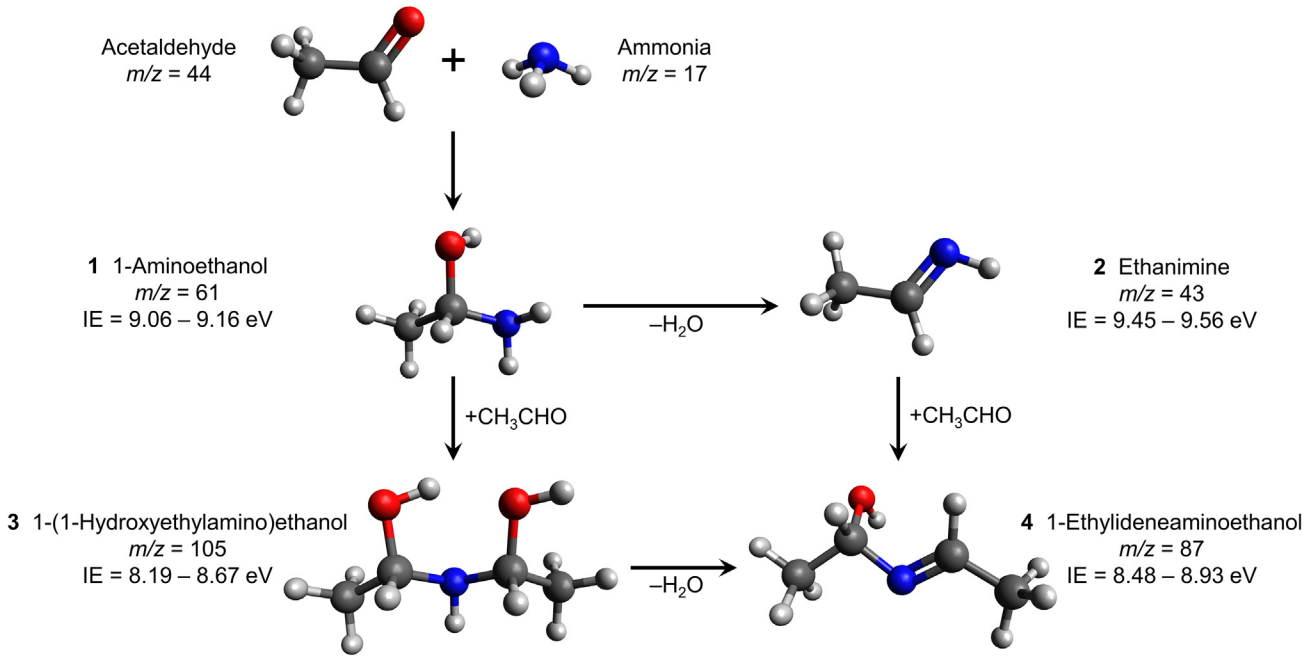

Figure 2. Thermal reactions of acetaldehyde and ammonia

Nucleophilic addition of ammonia to acetaldehyde results in the formation of experimentally detected 1-aminoethanol (**1**, $CH_3CH(OH)NH_3$), and subsequent addition of acetaldehyde forms 1-(1-hydroxyethylamino)ethanol (**3**, $NH(CH(OH)CH_3)_2$); subsequent dehydration of these products yields *E* or *Z* isomers of ethanimine (**2**, CH_3CHNH) and 1-ethylideneaminoethanol (**4**, $CH_3CH(OH)NCHCH_3$), respectively.

carbon monoxide (CO).[49] Although the cloud is quiescent, temperatures remain as low as 10 K,[50–52] and ices are chemically processed by ultraviolet (UV) radiation produced by protostars within the cloud and by GCRs[10,53,54]; thus, despite the low average temperatures, energetic initiation from these sources allows access to non-equilibrium chemistry. This process has been linked to the formation of a variety of COMs, and of particular interest here are carbonyl-containing molecules, such as aldehydes,[55–57] ketones,[58] and carboxylic acids,[59–62] which can act as electrophiles for thermal reactions with nucleophiles yielding prebiotic ligands as demonstrated here.

In contrast to the complex mixture of ice constituents found in the interstellar medium (ISM), these model ices consist of components selected from those molecules detected in the ISM—nucleophilic ammonia and electrophilic acetaldehyde (Table S1).[63,64] This simplified mixture facilitates the assessment of fundamental reaction mechanisms and the assignment of reaction products according to their FTIR spectra, ionization energies, mass-to-charge ratio (*m/z*), and isotopic effects on both FTIR spectra and *m/z*. Considering the use of simplified ice compositions, molecules formed in these laboratory experiments represent only a small number of the possible reaction products; conversely, molecules formed in these experiments are expected to form in interstellar ices where reactants are available. More broadly, the demonstration of a specific reaction mechanism in laboratory ices shows that the mechanism can operate in interstellar ices and demonstrates the possibility of any product of that mechanism. Here, we investigate the formation of **1** (Reaction 1) and consecutive reactions of **1** (Reactions 2, 3, 4A, and 4B) under conditions simulating the environment of molecular clouds during star formation and commensurate warming by observing changes in the ice that occur during temperature-programmed desorption (TPD). These experiments were designed to unravel the

Please cite this article in press as: Marks et al., Quantum-tunneling-mediated synthesis of prebiotic chelation agents in interstellar analog ices, Chem (2023), https://doi.org/10.1016/j.chempr.2023.07.003

mechanism of formation of **1** exploiting simplified polar model ices composed only of ammonia and acetaldehyde. Deposition below 10 K is followed by heating to 320 K at a rate of 1 K per min^{-1} simulating the temperature cycle experienced by ices in molecular clouds. Isotopic labeling was used to explore the kinetic isotope effect and aid in the assignment of FTIR spectra, in addition to assigning molecular formulas in mass spectrometry experiments exploiting isomer selective photoionization studies (PI-ReToF-MS).[65]

$$NH_3 + CH_3CHO \rightarrow CH_3CH(OH)NH_2\ (\mathbf{1}) \qquad \text{(Reaction 1)}$$

$$CH_3CH(OH)NH_2\ (\mathbf{1}) \rightarrow CH_3CHNH\ (\mathbf{2}) + H_2O \qquad \text{(Reaction 2)}$$

$$CH_3CH(OH)NH_2\ (\mathbf{1}) + CH_3CHO \rightarrow NH(CH(OH)CH_3)_2\ (\mathbf{3}) \qquad \text{(Reaction 3)}$$

$$NH(CH(OH)CH_3)_2\ (\mathbf{3}) \rightarrow CH_3CH(OH)NCHCH_3\ (\mathbf{4}) + H_2O \qquad \text{(Reaction 4A)}$$

$$CH_3CHNH\ (\mathbf{2}) + CH_3CHO \rightarrow CH_3CH(OH)NCHCH_3\ (\mathbf{4}) \qquad \text{(Reaction 4B)}$$

Infrared spectroscopy

FTIR spectra collected after the ice deposition revealed strong fundamentals of ammonia at 1,077 (ν_2), 3,394 (ν_3), and 1,627 cm^{-1} (ν_4).[66] For acetaldehyde, major peaks were detected at 3,006 (ν_1), 1,428 (ν_5), 1,350 (ν_7), and 1,128 cm^{-1} (ν_8) (Figures S1–S4).[67] Prior to the heating of the ice, no evidence is found to indicate the presence of any species other than the aforementioned reactants (Table S2). During the heating of the ice, sublimation of ammonia (105 K) and acetaldehyde (120 K) was observed, and the FTIR spectrum of the remaining residue was collected (Figure 3). The areas of the deconvoluted peaks were utilized to determine absorption coefficients for all bands observed (Table S3).[35] The absorption intensities were utilized to determine that the reaction had consumed approximately 2% of the reactants in the ice.[35] Experiments with deuterated ices ammonia-d_3-acetaldehyde (Figure S5), ammonia-acetaldehyde-d_4 (Figure S6), and ammonia-d_3-acetaldehyde-d_4 (Figure S7) were conducted; they permit an unambiguous assignment of OH, NH, and CH stretching modes. The hydrogen stretching region is deconvoluted into its component bands (Figure 3B), whereas the highest frequency absorptions are assigned to the NH stretches with the asymmetric mode at 3,354 cm^{-1} and symmetric mode at 3,286 cm^{-1}. Observation of the small peak near 3,200 cm^{-1} in all isotopically substituted ices indicates that this feature must be a combination band or overtone of a motion(s) that does not include hydrogen. The intensity and width of the band at 3,190 cm^{-1} are typical of an OH stretch in a polar environment where hydrogen bonding is prevalent. The CH stretching region contains three bands at 2,986, 2,935, and 2,879 cm^{-1}, which are all assigned to the motion of the methyl group, and the peak at 2,773 cm^{-1} is the result of CH stretching from the central carbon. Among the lower frequency vibrations (Figure 3C), NH bending is observed near 1,600 cm^{-1} and a series of peaks attributable to CH or OH bending modes are found at 1,400, 1,375, and 1,346 cm^{-1}. The overlapping bands for CC, CO,

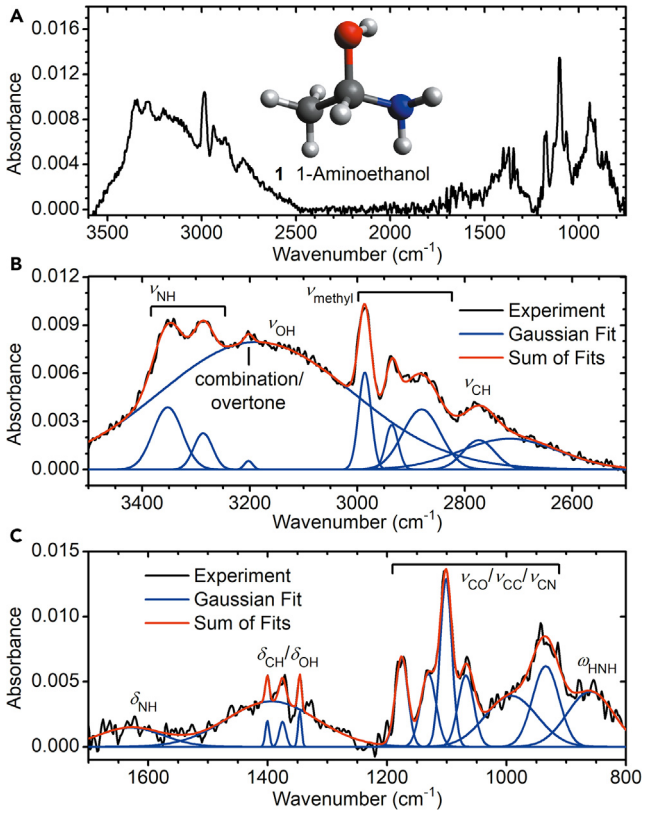

Figure 3. FTIR spectrum of acetaldehyde-ammonia ice

(A) Measured after sublimation of acetaldehyde and ammonia, which demonstrates excellent agreement with the spectrum of 1-aminoethanol.[35]

(B) The region 3,500–2,500 cm^{-1}, comprising NH, OH, and CH stretching modes, is shown magnified and deconvoluted.

(C) The region 1,700–800 cm^{-1}, comprising NH, OH, and CH bending modes in addition to CO, CC, and CN stretching modes, is also shown magnified and deconvoluted. Assignment labels: stretching (ν), bending (δ), rocking (ρ), inversion (ω).

and CN stretching are effectively indistinguishable and all fall within the range of 1,200 to 900 cm^{-1}.

The CO/CN stretching mode at 1,176 cm^{-1} is particularly useful for observing the formation of **1** *in situ* because it does not overlap with any absorption of the reactants. The CC stretching mode of **1**-d_7 at 1,231 cm^{-1} is observed in fully deuterated ammonia-d_3-acetaldehyde-d_4 ice. These bands were monitored during TPD of the fully deuterated and non-deuterated ices, and the observed intensities as a function of temperature are shown in Figure 4. At temperatures below 105 K, these two ices demonstrate substantially different reactivity, and non-deuterated ice shows a gradual increase in the intensity of FTIR signal assigned to **1**. This low-temperature absorption is linearly interpolated to determine the baseline intersect and indicates that the reaction starts at 65 $\pm$ 5 K. In deuterated ices, this signal is not observed until 105 $\pm$ 8 K. A reduction in the low-temperature reactivity ammonia and acetaldehyde upon deuteration is a clear example of the kinetic isotope effect and a strong indication that quantum tunneling may contribute to the reaction at low temperatures.[68]

The increasing infrared absorption, and therefore abundance, of **1** (Figure 4) shows that the limited mobility of the reactants within the solid does not prevent the

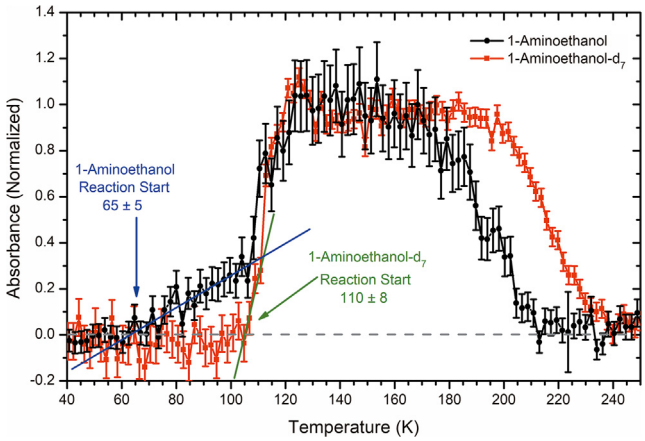

Figure 4. Abundance of 1-aminoethanol—the precursor to the prebiotic chelating agent 1-(1-hydroxyethylamino)ethanol ($NH(CH(OH)CH_3)_2$)—as a function of temperature

Integrated infrared absorption intensity (error bars show standard error) of selected peaks of 1-aminoethanol (1,176 cm^{-1}) and 1-aminoethanol-d_7 (1,231 cm^{-1}). The onset of 1-aminoethanol formation is interpolated by fitting its absorption at 60–110 K and the onset of 1-aminoethanol-d_7 formation used a fit to its absorption at 100–112 K.

reaction from proceeding. The rapid increase in reaction rate observed at 105–120 K in deuterated and undeuterated ices coincides with the sublimation of ammonia and acetaldehyde (Figure S8), and it is likely caused by the increased reactant mobility during sublimation. Upon complete sublimation of both reactants, **1** remains in the ice until it begins to sublime at 180, or 200 K for **1**-d_7. The increase in sublimation temperature for the deuterated product is likely the result of variations in molecular mass and hydrogen-bond strength.[69] Throughout these investigations, no FTIR absorptions are detected, which can be assigned to any other species, such as **2**, **3**, or **4**. Therefore, observation of these species requires more sensitive techniques than direct absorption spectroscopy.

PI-ReToF-MS

In these experiments, PI-ReToF-MS was used to mass-analyze and *isomer-specifically* detect sublimed molecules during TPD. A species can be detected only if the incident photon energy is in excess of molecular adiabatic ionization energy (Table S4).[70–73] Mass spectra obtained are plotted as a function of temperature in Figure 5. Substantial ion signal was collected with 10.49 eV photons for ions representing a wide range of masses, indicating a rich chemistry occurring during TPD. No signal was observed at the *m/z* channels investigated with photon energy of 8.90 eV, which shows that no species with an adiabatic ionization energy lower than this was produced in the studied ices at detectable concentrations. The computed adiabatic ionization energies reported in Figure 2 are presented as ranges that include ionization energies of all conformers (Tables S5, S6, and S7). The reaction scheme outlined in Figure 2 focuses on nucleophilic addition and dehydration, and these products do not isomerize at the low temperatures at which they are detected. This limits the possible molecular structures to those exhibited and provides an unambiguous identification, as demonstrated by the measurement of ionization energy, molecular mass, and molecular formula.

The signals collected for $m/z = 61$ with a range of photon energies as a function of temperature in ammonia-acetaldehyde ice are shown in Figure 6A. The observed signal demonstrates a bimodal profile with a minor peak at 120 K and a major

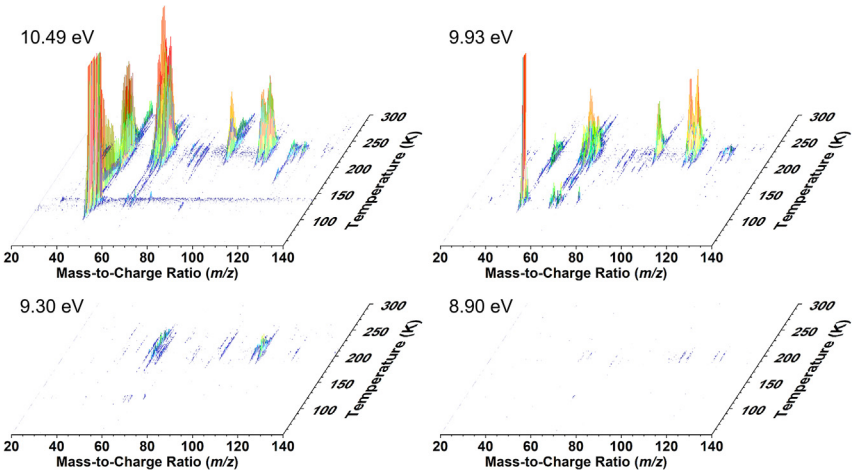

Figure 5. PI-ReToF mass spectra of ammonia-acetaldehyde ices

Mass spectra are shown as a function of temperature and mass-to-charge ratio (*m/z*) during the temperature-programmed desorption (TPD) of the analog ices with photoionization with a range of photon energies.

peak at 200 K. The minor peak coincides with sublimation of ammonia and acetaldehyde (Figure S8) and is likely the result of co-sublimation of **1**. Ions of **1** can be observed only when the photon energy is greater than the adiabatic ionization energy, computed to be 9.06–9.16 eV. Substantial signal is observed with 10.49 eV photons, and signal is still observed with photon energies of 9.93 and 9.30 eV. However, with 8.90 eV photons, no signal is observed; therefore, the ionization energy of the observed species must be between 8.90 and 9.30 eV, agreeing with the range computationally predicted for **1**. To support this assignment, isotopically substituted ices were studied, which contained ammonia-acetaldehyde-^{13}C, ammonia-acetaldehyde-d_3 (CD_3CHO), and ammonia-acetaldehyde-d_4 (Figure 6B). During the addition of ammonia to acetaldehyde, all atoms are conserved; therefore, the isotopic shift of acetaldehyde must directly correspond to a change in the mass of **1**. The signal observed at $m/z = 61$ is found to shift in response to isotopic labeling by an amount equal to the change in mass of the labeled acetaldehyde employed for each experiment. This confirms that the molecular formula must be C_2H_7NO and the molecule observed is **1**.

The calculated adiabatic ionization energy of **2** is 9.45–9.56 eV. This means that it can be ionized with photons of 10.49 and 9.93 eV, but not at 9.30 eV. This is observed experimentally in Figure 6C, where ions of $m/z = 43$ are observed with photons of 10.49 and 9.93 eV, but not at 9.30 eV. The observed signal must then be due to the presence of a molecule with an ionization energy between 9.30 and 9.93 eV. This signal is only 1 amu less than acetaldehyde, and a combination of saturation of the detection apparatus by the intense acetaldehyde signal and co-sublimation of **2** with the reactants results in a significant peak at 120 K when 10.49 eV photons are employed. This is also demonstrated by the region of dark blue lying along the temperature axis at 120 K for the PI-ReToF-MS mass spectra observed at 10.49 eV in Figure 5. The peak observed at 200 K coincides with the sublimation of **1**, and it is possible that predissociation of **1** due to its excess internal energy after photoionization could result in the elimination of water from the cation. However, if this were the case, the TPD profiles of **1** and **2** would be expected to be identical, which is not the case here. Addition of ammonia to acetaldehyde in Reaction 1 is expected to proceed via intramolecular proton transfer to form the hydroxy (–OH) moiety.

Please cite this article in press as: Marks et al., Quantum-tunneling-mediated synthesis of prebiotic chelation agents in interstellar analog ices, Chem (2023), https://doi.org/10.1016/j.chempr.2023.07.003

CellPress

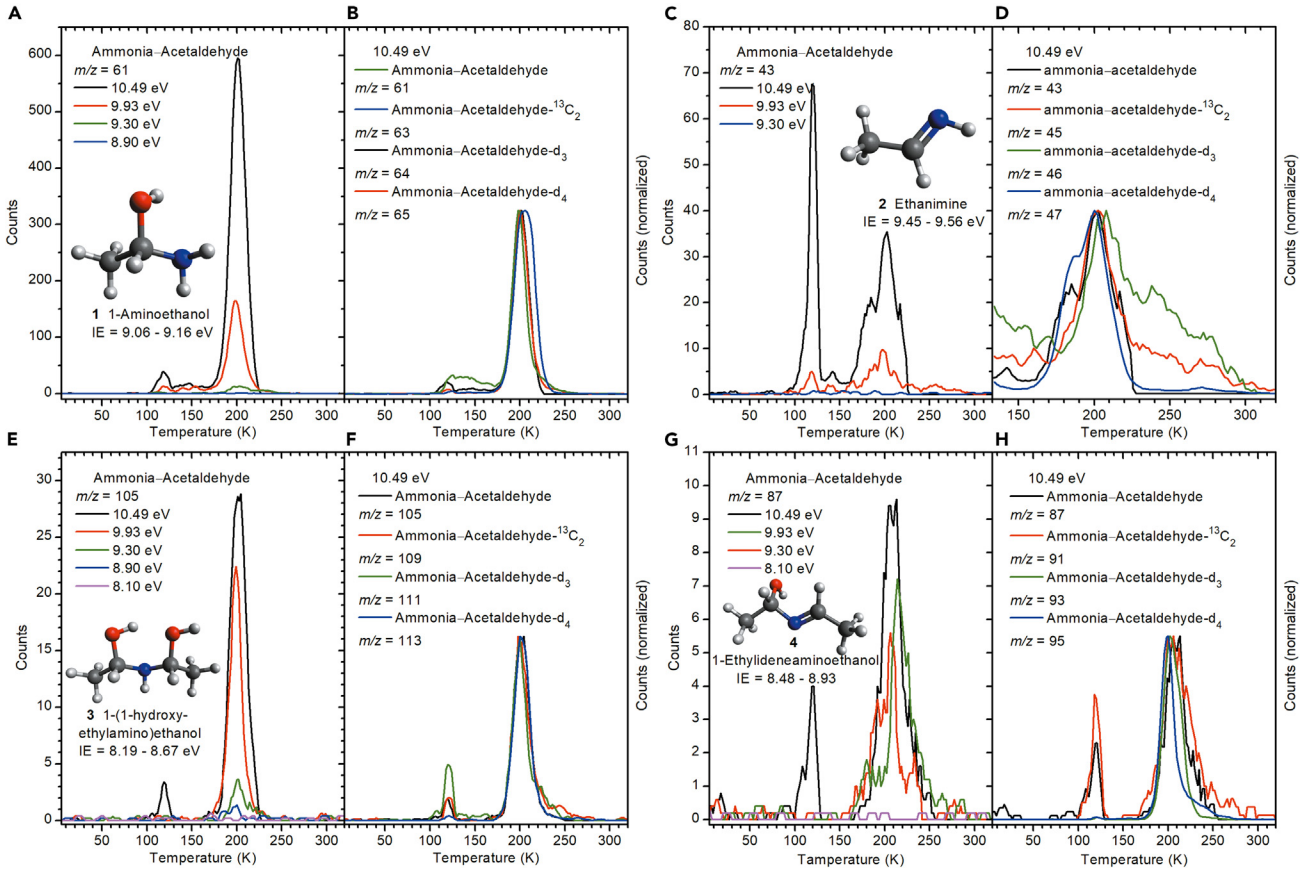

Figure 6. PI-ReToF-MS observation of molecules 1–4

(A–H) Ion signals measured during the temperature-programmed desorption (TPD) of ammonia-acetaldehyde ices (A) at m/z = 61 with a range of ionization photon energies, (B) at 10.49 eV for C_2H_7NO with isotopic substitution, (C) at m/z = 43 with a range of ionization photon energies, (D) at 10.49 eV for C_2H_5N with isotopic substitution, (E) at m/z = 105 with a range of ionization photon energies, (F) at 10.49 eV for $C_4H_{11}NO_2$ with isotopic substitution, (G) at m/z = 87 with a range of ionization photon energies, and (H) at 10.49 eV for C_4H_9NO with isotopic substitution.

Subsequent elimination of water (H_2O) in Reaction 2 requires transfer of a second hydrogen; therefore, both hydrogens eliminated in Reaction 2 originate from ammonia. The isotopic mass shift of acetaldehyde resulting from isotopic labeling of either the carbon or hydrogen in acetaldehyde must then directly correspond to a shift in **2** because these atoms are conserved through Reactions 1 and 2. The predicted isotopic shifts are seen experimentally (Figure 6D) and confirm the molecular formula to be C_2H_5N. The molecular formula in combination with the measured ionization energy permits clear assignment of this peak to **2**.

The predicted adiabatic ionization energy of **3** is 8.19–8.67 eV. This molecule can be ionized with photons of 8.90 eV or higher, but at 8.10 eV it cannot be ionized. Ions are detected at m/z = 105 from ammonia-acetaldehyde ices studied with 10.49, 9.93, 9.30, and 8.90 eV photons (Figure 6E). Similar to **2**, this molecule is found to sublime at 200 K with the sublimation of **1**. When a photon energy of 8.10 eV is used, no signal is observed, which limits the ionization energy of the observed molecule to 8.10–8.90 eV, within the range predicted for **3**. Because Reaction 3 requires initial formation of **1**, it conserves all atoms that are present in one ammonia and two acetaldehyde molecules; therefore, the isotopic mass shift resulting from labeling of acetaldehyde will result in twice the shift for **3**. This is observed in isotopic substitution experiments (Figure 6F), which show that signal is consistently observed for the

Please cite this article in press as: Marks et al., Quantum-tunneling-mediated synthesis of prebiotic chelation agents in interstellar analog ices, Chem (2023), https://doi.org/10.1016/j.chempr.2023.07.003

peak at 200 K which is shifted by twice the mass of the isotopically labeled acetaldehyde. This confirms the molecular formula to be $C_4H_{11}NO_2$ and is assigned to **3**.

The predicted adiabatic ionization of **4** is 8.43–8.93 eV. This should result in its observation with photons of 9.30 eV or higher energy, but no signal should be observed at 8.10 eV. Experimentally, signal is observed with m/z = 87 with 10.49, 9.93, and 9.30 eV, but no signal is observed at 8.10 eV (Figure 6G). Although **4** can be formed in Reaction 4A or 4B, either of these reaction sequences results in the addition of ammonia to two acetaldehyde molecules and the elimination of water. Both hydrogens eliminated in the water originate from ammonia; therefore, the isotopic shift resulting from labeling of the carbon or hydrogens of acetaldehyde should result in twice the isotopic shift being exhibited by **4**. This was observed experimentally (Figure 6H) and provides confirmation of a C_4H_9NO molecular formula and verifies the observation of **4**.

Reaction mechanism and computational quantum chemistry

Quantum chemical calculations were performed to explore the potential energy surface (PES) of the addition of ammonia to acetaldehyde (Figure 7A). This reaction commences with an ammonia-acetaldehyde complex, which faces a 124 kJ mol^{-1} barrier to the formation of **1** (Reaction 1). The addition of ammonia to acetaldehyde is predicted to proceed by a concerted mechanism. The initial non-covalent complex undergoes C–N bond formation simultaneously with proton transfer to yield **1** (Figures S9–S12). The identified transition state in the calculated PES displays the process of proton transfer, in which a hydrogen is partially bonded to both N and O.[29] Microsolvation, the full quantum chemical treatment of a limited number of solvent molecules, is accomplished here with the inclusion of one (Figure 7B) and two (Figure 7C) additional ammonia molecules. All calculations implicitly took into account the presence of solid ammonia as the solvent. The addition of only one ammonia results in a reduction of the reaction barrier for Reaction 1 to only 28 kJ mol^{-1} and is accompanied by a stabilization of **1** relative to the initial reactant complex from 13 kJ mol^{-1} in the implicit solvent to 62 kJ mol^{-1} with two explicit solvent molecules. Inclusion of two ammonia molecules does not significantly alter the reaction energetics further. A similar pattern is identified for elimination of water from **1** (Reaction 2), where inclusion of only one additional ammonia results in a reduction of the reaction barrier, but the second solvating ammonia has a negligible effect. The transition states for Reactions 1 and 2 both demonstrate stabilization by solvent-assisted proton transfer. It is likely that these calculations may overestimate the real barrier for these reactions, as evidenced by the rapid increase in the formation of **1** exhibited by both deuterated and undeuterated ices at temperatures above 110 K (Figure 4). This change in reaction rate likely represents the crossover temperature at which the reaction transitions from quantum tunneling (through the barrier) to thermodynamic (over the barrier) control. This temperature does not represent a sufficient amount of thermal energy for a reaction with a 26 kJ mol^{-1} barrier to proceed, and this discrepancy may result from the simplification that makes these calculations practical, e.g., implicit solvent modeling and, possibly, a limited number of microsolvating molecules. Reaction 2 has a larger barrier on the order of 160 kJ mol^{-1}, which is anticipated to result in a low rate of formation and explains the low intensity with which this molecule was observed. Single photon ionization is a highly sensitive technique and was only able to detect **2** in quantities several orders of magnitude less than that of **1**. It should be noted that dehydration reactions in ices have been shown to accelerate under acid catalysis and are strongly dependent on pH, the low quantity of **2** observed may be the result of the basicity of an ice comprised largely of ammonia.[37,40,41]

Please cite this article in press as: Marks et al., Quantum-tunneling-mediated synthesis of prebiotic chelation agents in interstellar analog ices, Chem (2023), https://doi.org/10.1016/j.chempr.2023.07.003

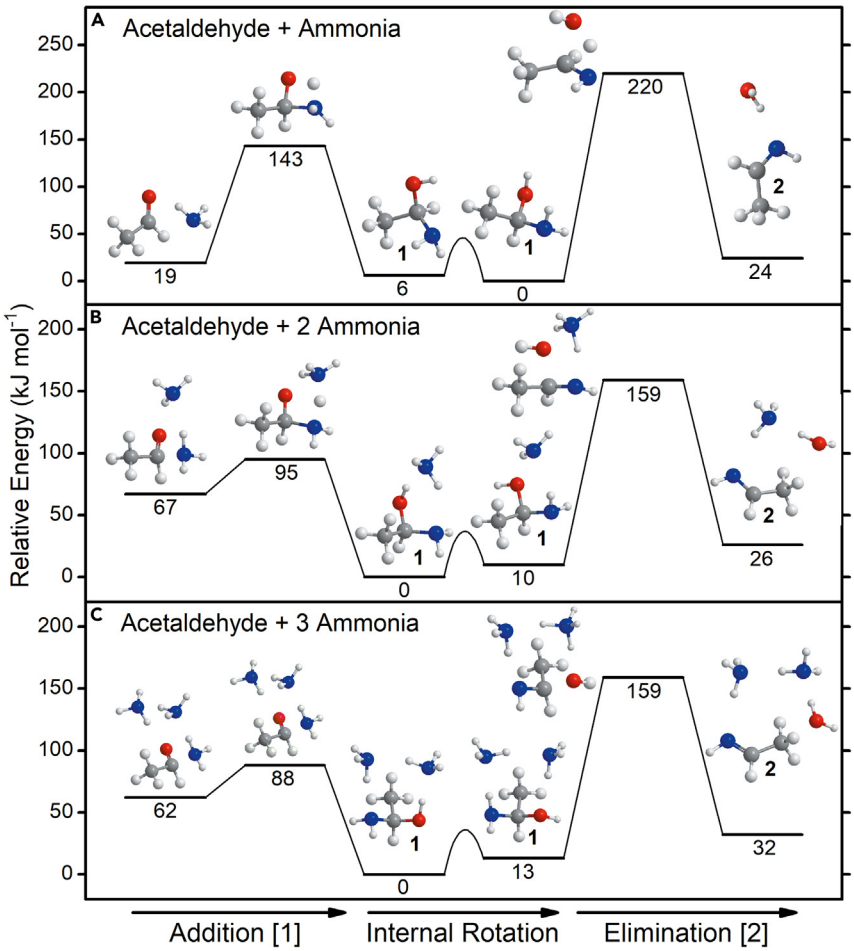

Figure 7. Effects of microsolvation on reactions of acetaldehyde and ammonia

(A–C) Potential energy surface for the addition of ammonia to acetaldehyde (Reaction 1) to produce **1** and subsequent elimination of water (Reaction 2) to produce **2**. (A) The reaction in presence of only implicit solid ammonia solvent in the form of a dipole field demonstrates a much higher barrier to addition than those calculated with microsolvation by (B) one or (C) two additional ammonia molecules.

The barrier to addition of **1** to acetaldehyde, Reaction 3, is found to be reduced with each additional explicitly solvating ammonia from 137 kJ mol^{-1} in the implicit solid ammonia solvent to only 14 kJ mol^{-1} with three solvent molecules directly involved in the reaction (Figures 8 and S13–S16). Similarly, the relative stability of **3** compared with the reactants increases with each successive solvating ammonia up to a maximum of 60 kJ mol^{-1} with three explicit solvent molecules. In contrast to this behavior, with increasing microsolvation the barrier to the dehydration of **3**, Reaction 4A, is not substantially impacted by the inclusion of solvating ammonia after the inclusion of the first solvent molecule. Similar to Reaction 2, Reaction 4A has a large barrier and the formation in basic ices studied here must proceed slowly. Reaction 4B was not considered in these computationally expensive calculations because imines (RNH) are typically less nucleophilic than amines, and although possible, this is a less likely route to the formation of **4** at these low temperatures.[28]

Prebiotic chelating agents

Substituents containing an electronegative atom, e.g., oxygen-containing alcohols and nitrogen-containing amines, have localized negative charges in their

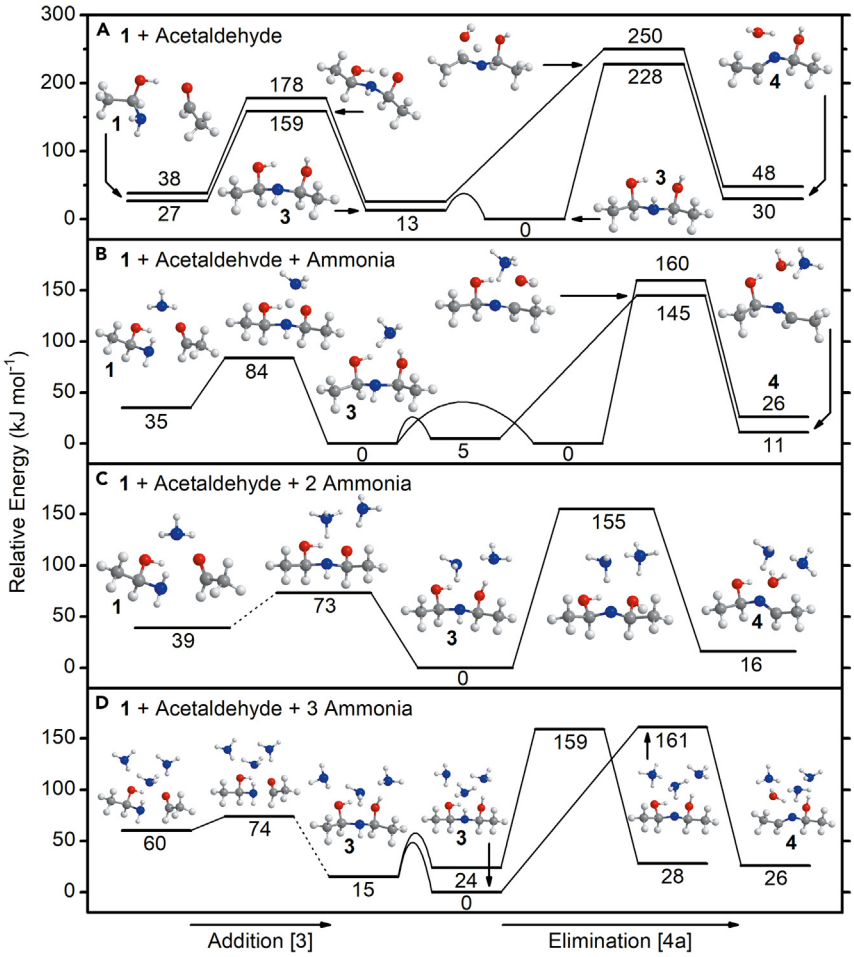

Figure 8. Effects of microsolvation on reactions of 1-aminoethanol and ammonia

(A–D) Potential energy surface for the addition of **1** to acetaldehyde to produce **3** (Reaction 3) and subsequent elimination of water to produce **4** (Reaction 4A). The reaction (A) in presence of only implicit solid ammonia solvent demonstrates a much larger barrier to addition than those calculated with microsolvation by (B) one, (C) two, or (D) three additional ammonia molecules.

nonbonding electrons.[74] These orbitals can readily participate in coordination bonds with metal cations via the donation of electron density from non-bonding pairs to the metal cation. Furthermore, **3** and the other complex product molecules proposed in Figure 1 contain multiple substituent groups with non-bonding electrons and can bond as polydentate ligands in which they form multiple bonds to a metal cation. The energetics of chelation by molecules containing hydroxy and secondary amino moieties in an aqueous environment were studied by calculating the binding energy and Gibbs free energy of **3** to Na^+, K^+, Mg^{2+}, and Ca^{2+} by substitution for water in the fully coordinated hexahydrate complexes (Figures 9 and S17–S21). The calculated free energies of reaction for Reactions 5, 6, and 7 can be used to assess the variations in binding energy relative to water of the different coordinating moieties of **3** to the metal cation (M^{n+} = Na^+, K^+, Mg^{2+}, and Ca^{2+}) with calculations that incorporate a semi-empirical solvent model to account for the energy of solvation at 298.15 K.[75]

$$\mathbf{3} + M^{n+}(H_2O)_6 \rightarrow M^{n+}(\mathbf{3})(H_2O)_4 + 2(H_2O) \qquad \text{(Reaction 5)}$$

Please cite this article in press as: Marks et al., Quantum-tunneling-mediated synthesis of prebiotic chelation agents in interstellar analog ices, Chem (2023), https://doi.org/10.1016/j.chempr.2023.07.003

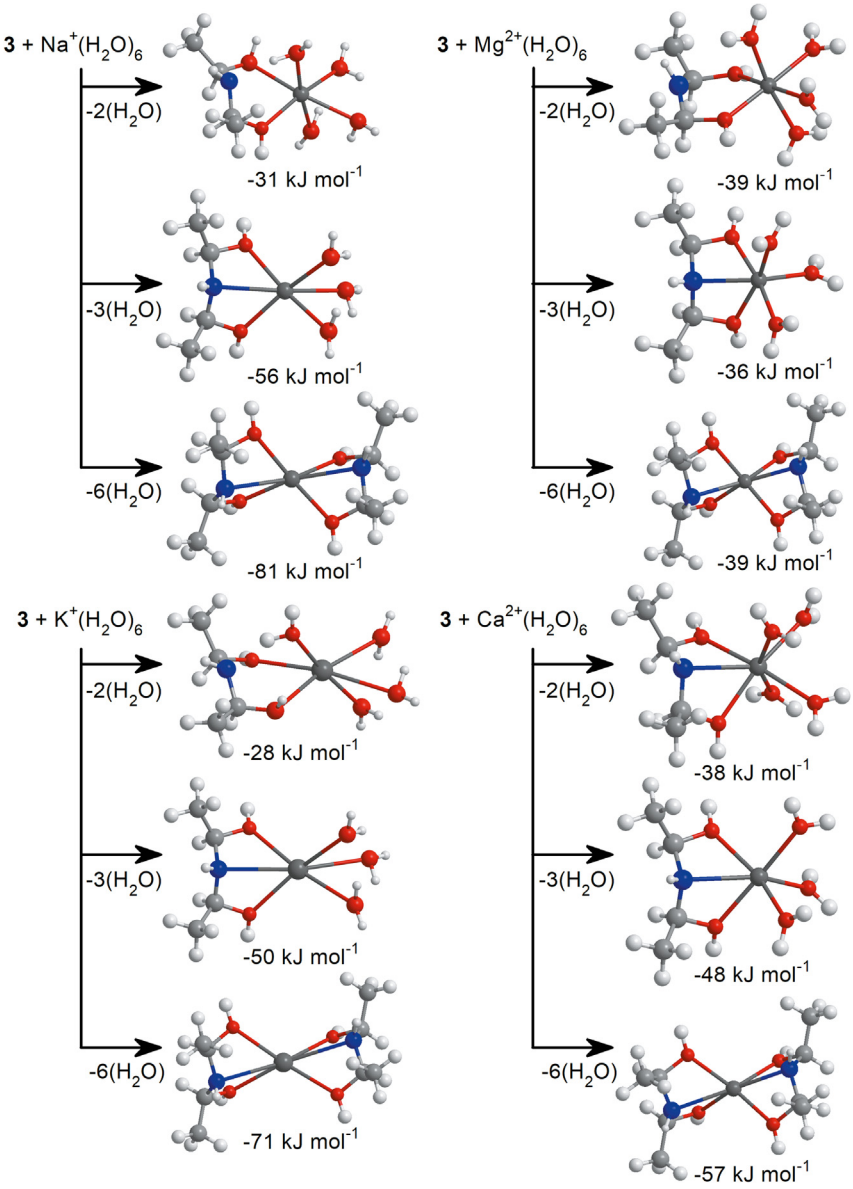

Figure 9. Gibbs free energy of reaction for chelation of biologically relevant ions

Chelation of fully coordinated metal ions (Na^+, K^+, Mg^{2+}, and Ca^{2+}) by substitution of water for **3**. Gibbs free energies of reaction computed at 298.15 K in aqueous solution are those that result from substitution of two, three, or six water molecules by **3** to form 6-coordinate complexes.

$$\mathbf{3} + M^{n+}(H_2O)_6 \rightarrow M^{n+}(\mathbf{3})(H_2O)_3 + 3(H_2O) \qquad \text{(Reaction 6)}$$

$$2(\mathbf{3}) + M^{n+}(H_2O)_6 \rightarrow M^{n+}(\mathbf{3})_2 + 6(H_2O) \qquad \text{(Reaction 7)}$$

For $Na^+(H_2O)_6$, displacement of two water ligands in Reaction 5 allows **3** to bind through both hydroxyl groups in a bidentate configuration. This process is exoergic by 31 kJ mol^{-1}, which shows that the O–Na^+ interactions are stronger with the hydroxyl groups of **3** than with water by 15.5 kJ mol^{-1} each. Displacement of an additional water ligand by the amine of **3** in Reaction 6 permits the formation of an N–Na^+

Please cite this article in press as: Marks et al., Quantum-tunneling-mediated synthesis of prebiotic chelation agents in interstellar analog ices, Chem (2023), https://doi.org/10.1016/j.chempr.2023.07.003

dative bond, which is exoergic by 56 kJ mol^{-1}. This increase in reaction free energy from Reaction 5 to Reaction 6 by 25 kJ mol^{-1} is due only to the addition of interactions between nitrogen and the metal. Reaction 7 includes replacement of all water ligands with two molecules of **3**; this reaction is predicted to be exoergic by 81 kJ mol^{-1}. The binding free energy of two ligands is not found to be simply twice that of a single ligand, which is in part due to the decreased energy of solvation. The complex resulting from full complexation by two molecules of **3** has several non-polar methyl groups, which would decrease water solubility but aid solvation in non-polar environments. The energetics of the bonding of **3** to K^+ demonstrate a similar pattern in the relative free energies of reaction to those of Na^+, although the K^+ complexes tend to exhibit slightly lower reaction energies than the equivalent Na^+ complexes.

For alkali metal cations Na^+ and K^+, the coordination bond with nitrogen is stronger than the equivalent bond with oxygen. In comparison with the alkaline earth metals, the O–Mg^{2+} and O–Ca^{2+} bonds formed in Reaction 5 are stronger than those exhibited by either Na^+ or K^+ with a total free energy of reaction of 39 kJ mol^{-1}, or 19.5 kJ mol^{-1} for each bonding interaction. The N–Mg^{2+} bond formed in Reaction 6 results in a less exoergic reaction than in Reaction 5, demonstrating that the tridentate bonding configuration is not favorable thermodynamically. Formation of the same nitrogen bond to Ca^{2+} in Reaction 6 increases the exoergicity of the reaction by only 10 kJ mol^{-1}, and although this is thermodynamically sound, it is not a strong bond relative to those of the hydroxyl moieties. Reaction 7 exhibits only a small increase in reaction energy relative to Reaction 6 with the alkaline earth metal cations. However, a significant portion of reaction energy is lost in Reaction 7 because of a commensurate decrease in solvation energy, consistent with the chelation of a highly polarizing dication in an aqueous environment.

Conclusions

The very first laboratory observation of 1-(1-hydroxyethylamino)ethanol (**3**, $NH(CH(OH)CH_3)_2$) is demonstrated here through quantum tunneling in an interstellar analog ice under thermal conditions and reveals a plausible mechanism of formation for multi-functionalized complex organics in deep space, which may act as prebiotic chelating agents that were once delivered to early Earth by meteorite and comets. This accomplishment was achieved through the exploitation of the PI-ReToF-MS technique revealing a facile preparation of **3** at or below 105–120 K. The detection of **3** is corroborated by isotopic substitution experiments also demonstrating the conservation of all four hydrogens incorporated from the acetaldehyde reactant. Supported further by quantum chemical calculations, the complex chain of Reactions 1, 2, 3, and 4A was shown to proceed via transfer of hydrogen from ammonia and/or the amine involving intramolecular proton transfer in **2**–**4** (Figure S9). Further evidence of the underlying reaction mechanism is provided by FTIR spectroscopy, and the lack of low temperature (<105 K) formation of **1** in fully deuterated ice not only indicates that hydrogen/deuterium transfer is operating but also that the proton transfer can occur by quantum tunneling through the initial barrier to addition of ammonia to acetaldehyde. The quantum chemical investigation of this reaction shows that increasing microsolvation reduces the activation barrier for the formation of **1** due to the protic and basic nature of ammonia molecules acting as intermediary in the proton transfer. Although the barriers for Reactions 2 and 4A are not as significantly impacted by solvation, these are dehydration reactions, and although they are expected to have strongly pH-dependent reaction rates, this property bears further study. Ices employed in these experiments contained only ammonia and acetaldehyde to permit a mechanistic analysis; however, these results

Please cite this article in press as: Marks et al., Quantum-tunneling-mediated synthesis of prebiotic chelation agents in interstellar analog ices, Chem (2023), https://doi.org/10.1016/j.chempr.2023.07.003

serve as a basis on which a greater understanding of thermal reactions in ices can be built by assessing the effects of pH and of introducing more abundant interstellar ice components, such as water, methanol, carbon monoxide, and carbon dioxide.

These experiments mark a vital starting point in understanding the availability of chelation agents of interstellar origin to prebiotic chemistry, synthesized in the interstellar medium at temperatures as low as 65 $\pm$ 5 K. Eventually delivered to early Earth, metal chelation (Na^+, K^+, Mg^{2+}, and Ca^{2+}) through the moieties of **3** is demonstrated computationally to be favorable in aqueous solution, mimicking the early ocean on Earth. Although endoergic at 0 K, at 298 K, these chelating reactions are driven by the entropy factor, resulting in reactions exoergic by up to 81 kJ mol^{-1} (Figure 9). The facile chelation of solvated metal cations by **3** in an aqueous environment is essentially propelled by strong tridentate bonds to alkali metal cations and bidentate bonds to alkaline earth metal cations. The chelated metal complexes carry up to four non-polar methyl (CH_3) moieties, thus aiding the compatibility of these complexes with non-polar environments, such as the interstitial layers of (prebiotic) phospholipid membranes. The demonstrated ability of **3** to bond to Mg^{2+}, particularly through its hydroxy moieties, is of vital importance, considering its catalytic effect on RNA replication.[16–18,24]

Overall, the chelation agent **3** serves as a critical prototype for alike molecules that can potentially form via thermal processing of interstellar ices through an analogous mechanism involving more chemically complex aldehydes and amines. Despite its—by astronomical standards—high complexity, **3** represents one of the simplest structures feasible through nucleophilic addition in interstellar ices. The process of star formation from a molecular cloud can take up to 10^6 years. Once the protostar switches on, it warms the surrounding dust and ices contained in the star-forming region allowing the synthesis of **3**.[45] These chemicals represent the basic ingredients of the formation of solar systems from the protoplanetary disc, during which at least a fraction of the organics can be eventually incorporated into planetesimals. Once delivered to proto-Earth by comets and meteorites, the chelation agents are seeded into the oceans of early Earth, thus permitting their enduring presence in the environment in which primitive lifeforms were developing.[15] Chelation by **3** and similar molecules would have promoted the development of life by enabling ion transport in primitive cells, enabling the development of biological functions in which metallic ions are necessary.

EXPERIMENTAL PROCEDURES

Resource availability

Lead contact

Further information and requests for resources should be directed to and will be fulfilled by the lead contact, Ralf I. Kaiser (ralfk@hawaii.edu).

Materials availability

This study did not generate new unique reagents.

Data and code availability

The datasets generated during this study are available upon request.

SUPPLEMENTAL INFORMATION

Supplemental information can be found online at https://doi.org/10.1016/j.chempr.2023.07.003.

ACKNOWLEDGMENTS

The experiments at the University of Hawaii were supported by the US National Science Foundation (NSF), Division for Astronomy (NSF-AST 1800975). The W.M. Keck Foundation and the University of Hawaii at Manoa financed the construction of the experimental setup. The calculations of adiabatic ionization energies, reaction PESs, and chelation reaction energies were supported by the Ministry of Higher Education and Science of the Russian Federation via grant 075-15-2021-597. We acknowledge Ms. Joni Spencer for initial calculations of PES for the reaction of ammonia with acetaldehyde.

AUTHOR CONTRIBUTIONS

R.I.K. designed the experiments and directed the overall project. J.H.M. and J.W. performed all experiments with the assistance of A.M.T., and N.F.K. assisted in experiments where temperature-dependent FTIR data were collected. M.M.E., O.V.K., and I.O.A. calculated adiabatic ionization energies for all conformers of molecules **1**–**4**. A.A.N. and A.M.M. calculated the reaction potential energy surfaces and Gibbs free energies of chelation reactions, and A.M.M. supervised these calculations. J.H.M. prepared figures, analyzed experimental data, and co-wrote the manuscript with R.I.K.

DECLARATION OF INTERESTS

The authors declare no competing interests.

Received: March 24, 2023
Revised: June 6, 2023
Accepted: July 11, 2023
Published: August 9, 2023

REFERENCES

1. Orgel, L.E. (1968). Evolution of the genetic apparatus. J. Mol. Biol. *38*, 381–393. https://doi.org/10.1016/0022-2836(68)90393-8.

2. Crick, F.H.C. (1968). The origin of the genetic code. J. Mol. Biol. *38*, 367–379. https://doi.org/10.1016/0022-2836(68)90392-6.

3. Gilbert, W. (1986). Origin of life: the RNA World. Nature *319*, 618. https://doi.org/10.1038/319618a0.

4. Orgel, L.E. (2004). Prebiotic chemistry and the origin of the RNA World. Crit. Rev. Biochem. Mol. Biol. *39*, 99–123. https://doi.org/10.1080/10409230490460765.

5. Nuevo, M., Materese, C.K., and Sandford, S.A. (2014). The photochemistry of pyrimidine in realistic astrophysical ices and the production of nucleobases. Astrophys. J. *793*, 125. https://doi.org/10.1088/0004-637x/793/2/125.

6. Holtom, P.D., Bennett, C.J., Osamura, Y., Mason, N.J., and Kaiser, R.I. (2005). A combined experimental and theoretical study on the formation of the amino acid glycine (NH_2CH_2COOH) and its isomer ($CH_3NHCOOH$) in extraterrestrial ices. Astrophys. J. *626*, 940–952. https://doi.org/10.1086/430106.

7. Turner, A.M., Abplanalp, M.J., Blair, T.J., Dayuha, R., and Kaiser, R.I. (2018). An infrared spectroscopic study toward the formation of alkylphosphonic acids and their precursors in extraterrestrial environments. Astrophys. J. Suppl. Ser. *234*, 6. https://doi.org/10.3847/1538-4365/aa9183.

8. Turner, A.M., Abplanalp, M.J., Bergantini, A., Frigge, R., Zhu, C., Sun, B.-J., Hsiao, C.T., Chang, A.H.H., Meinert, C., and Kaiser, R.I. (2019). Origin of alkylphosphonic acids in the interstellar medium. Sci. Adv. *5*, eaaw4307. https://doi.org/10.1126/sciadv.aaw4307.

9. Ehrenfreund, P., and Charnley, S.B. (2000). Organic molecules in the interstellar medium, comets, and meteorites: a voyage from dark clouds to the early Earth. Annu. Rev. Astron. Astrophys. *38*, 427–483. https://doi.org/10.1146/annurev.astro.38.1.427.

10. Öberg, K.I. (2016). Photochemistry and astrochemistry: photochemical pathways to interstellar complex organic molecules. Chem. Rev. *116*, 9631–9663. https://doi.org/10.1021/acs.chemrev.5b00694.

11. Öberg, K.I., Boogert, A.C.A., Pontoppidan, K.M., van den Broek, S., van Dishoeck, E.F., Bottinelli, S., Blake, G.A., and Evans, N.J. (2011). The Spitzer ice legacy: ice evolution from cores to protostars. Astrophys. J. *740*, 109. https://doi.org/10.1088/0004-637x/740/2/109.

12. Boss, A.P. (1998). Temperatures in protoplanetary disks. Annu. Rev. Earth Planet. Sci. *26*, 53–80. https://doi.org/10.1146/annurev.earth.26.1.53.

13. Oró, J. (1961). Comets and the formation of biochemical compounds on the primitive Earth. Nature *190*, 389–390. https://doi.org/10.1038/190389a0.

14. Chyba, C., and Sagan, C. (1992). Endogenous production, exogenous delivery and impact-shock synthesis of organic molecules: an inventory for the origins of life. Nature *355*, 125–132. https://doi.org/10.1038/355125a0.

15. Kadoya, S., Krissansen-Totton, J., and Catling, D.C. (2020). Probable cold and alkaline surface environment of the Hadean earth caused by impact ejecta weathering. Geochem. Geophys. Geosyst. *21*, e2019GC008734. https://doi.org/10.1029/2019gc008734.

16. Monnard, P.A., and Szostak, J.W. (2008). Metal-ion catalyzed polymerization in the eutectic phase in water-ice: A possible approach to template-directed RNA polymerization. J. Inorg. Biochem. *102*, 1104–1111. https://doi.org/10.1016/j.jinorgbio.2008.01.026.

17. Szostak, J.W. (2012). The eightfold path to non-enzymatic RNA replication. J. Syst. Chem. *3*, 2. https://doi.org/10.1186/1759-2208-3-2.

18. Szostak, J.W. (2017). The narrow road to the deep past: in search of the chemistry of the origin of life. Angew. Chem. Int. Ed. Engl. *56*,

11037–11043. https://doi.org/10.1002/anie.201704048.

19. Pressman, A., Blanco, C., and Chen, I.A. (2015). The RNA World as a model system to study the origin of life. Curr. Biol. *25*, R953–R963. https://doi.org/10.1016/j.cub.2015.06.016.

20. Deamer, D. (2017). The role of lipid membranes in life's origin. Life (Basel) *7*, 5. https://doi.org/10.3390/life7010005.

21. Saha, R., Verbanic, S., and Chen, I.A. (2018). Lipid vesicles chaperone an encapsulated RNA aptamer. Nat. Commun. *9*, 2313. https://doi.org/10.1038/s41467-018-04783-8.

22. Cooper, G. (2018). The Cell: A Molecular Approach, Eighth Edition (Sinauer Associates).

23. Kolb, V.M. (2019). Handbook of Astrobiology, First Edition (CRC Press).

24. Adamala, K., and Szostak, J.W. (2013). Nonenzymatic template-directed RNA synthesis inside model protocells. Science *342*, 1098–1100. https://doi.org/10.1126/science.1241888.

25. Bakker, E.P. (1992). Alkali Cation Transport Systems in Prokaryotes, First Edition (CRC Press).

26. Augustine, G.J. (2004). Channels and Transporters. In Neuroscience, D. Purves, G.J. Augustine, D. Fitzpatrick, W.C. Hall, A.-S. LaMantia, J.O. McNamara, and S.M. Williams, eds. (Sinauer Associates), pp. 69–92.

27. Kawakami, K., Ohta, T., Nojima, H., and Nagano, K. (1986). Primary structure of the alpha-subunit of human na,K-ATPase deduced from cDNA sequence. J. Biochem. *100*, 389–397. https://doi.org/10.1093/oxfordjournals.jbchem.a121726.

28. Tuguldurova, V.P., Fateev, A.V., Malkov, V.S., Poleshchuk, O.K., and Vodyankina, O.V. (2017). Acetaldehyde-ammonia interaction: a DFT study of reaction mechanism and product identification. J. Phys. Chem. A *121*, 3136–3141. https://doi.org/10.1021/acs.jpca.7b00823.

29. Carey, F.A., and Sundberg, R.A. (2007). Advanced Organic Chemistry. Part A: Structure and Mechanisms, Fifth Edition (Springer).

30. Frasco, D.L. (1964). Infrared spectra of ammonium carbamate and deuteroammonium carbamate. J. Chem. Phys. *41*, 2134–2140. https://doi.org/10.1063/1.1726217.

31. Bossa, J.B., Borget, F., Duvernay, F., Theulé, P., and Chiavassa, T. (2008). Formation of neutral methylcarbamic acid ($CH_3NHCOOH$) and methylammonium methylcarbamate [$CH_3NH_3^+$][$CH_3NHCO_2^-$] at low temperature. J. Phys. Chem. A *112*, 5113–5120. https://doi.org/10.1021/jp800723c.

32. Bossa, J.B., Theulé, P., Duvernay, F., Borget, F., and Chiavassa, T. (2008). Carbamic acid and carbamate formation in NH_3:CO_2 ices – UV irradiation versus thermal processes. Astron. Astrophys. *492*, 719–724. https://doi.org/10.1051/0004-6361:200810536.

33. Bossa, J.-B., Duvernay, F., Theulé, P., Borget, F., d'Hendecourt, L., and Chiavassa, T. (2009). Methylammonium methylcarbamate thermal formation in interstellar ice analogs: A glycine salt precursor in protostellar environments. Astron. Astrophys. *506*, 601–608. https://doi.org/10.1051/0004-6361/200912850.

34. Bossa, J.B., Theule, P., Duvernay, F., and Chiavassa, T. (2009). NH_2CH_2OH Thermal Formation in Interstellar Ices Contribution to the 5–8 μm Region Toward Embedded Protostars. Astrophys. J. *707*, 1524–1532. https://doi.org/10.1088/0004-637x/707/2/1524.

35. Duvernay, F., Dufauret, V., Danger, G., Theulé, P., Borget, F., and Chiavassa, T. (2010). Chiral molecule formation in interstellar ice analogs: alpha-aminoethanol $NH_2CH(CH_3)OH$. Astron. Astrophys. *523*, A79. https://doi.org/10.1051/0004-6361/201015342.

36. Danger, G., Borget, F., Chomat, M., Duvernay, F., Theulé, P., Guillemin, J.-C., Le Sergeant d'Hendecourt, L.L.S., and Chiavassa, T. (2011). Experimental investigation of aminoacetonitrile formation through the Strecker synthesis in astrophysical-like conditions: reactivity of methanimine (CH_2NH), ammonia (NH_3), and hydrogen cyanide (HCN). Astron. Astrophys. *535*, A47. https://doi.org/10.1051/0004-6361/201117602.

37. Vinogradoff, V., Duvernay, F., Danger, G., Theulé, P., and Chiavassa, T. (2011). New insight into the formation of hexamethylenetetramine (HMT) in interstellar and cometary ice analogs. Astron. Astrophys. *530*, A128. https://doi.org/10.1051/0004-6361/201116688.

38. Vinogradoff, V., Duvernay, F., Danger, G., Theulé, P., Borget, F., and Chiavassa, T. (2013). Formaldehyde and methylamine reactivity in interstellar ice analogues as a source of molecular complexity at low temperature. Astron. Astrophys. *549*, A40. https://doi.org/10.1051/0004-6361/201219974.

39. Danger, G., Duvernay, F., Theulé, P., Borget, F., and Chiavassa, T. (2012). Hydroxyacetonitrile ($HOCH_2CN$) formation in astrophysical conditions. Competition with the Aminomethanol, a glycine precursor. Astrophys. J. *756*, 11. https://doi.org/10.1088/0004-637x/756/1/11.

40. Vinogradoff, V., Duvernay, F., Farabet, M., Danger, G., Theulé, P., Borget, F., Guillemin, J.C., and Chiavassa, T. (2012). Acetaldehyde solid state reactivity at low temperature: formation of the acetaldehyde ammonia trimer. J. Phys. Chem. A *116*, 2225–2233. https://doi.org/10.1021/jp3000653.

41. Vinogradoff, V., Rimola, A., Duvernay, F., Danger, G., Theulé, P., and Chiavassa, T. (2012). The mechanism of hexamethylenetetramine (HMT) formation in the solid state at low temperature. Phys. Chem. Chem. Phys. *14*, 12309–12320. https://doi.org/10.1039/c2cp41963g.

42. Noble, J.A., Theule, P., Borget, F., Danger, G., Chomat, M., Duvernay, F., Mispelaer, F., and Chiavassa, T. (2013). The thermal reactivity of HCN and NH_3 in interstellar ice analogues. Mon. Not. R. Astron. Soc. *428*, 3262–3273. https://doi.org/10.1093/mnras/sts272.

43. Theulé, P., Duvernay, F., Danger, G., Borget, F., Bossa, J.B., Vinogradoff, V., Mispelaer, F., and Chiavassa, T. (2013). Thermal reactions in interstellar ice: A step towards molecular complexity in the interstellar medium. Adv. Space Res. *52*, 1567–1579. https://doi.org/10.1016/j.asr.2013.06.034.

44. Agúndez, M., and Wakelam, V. (2013). Chemistry of dark clouds: databases, networks, and models. Chem. Rev. *113*, 8710–8737. https://doi.org/10.1021/cr4001176.

45. Carroll, B.W., and Ostlie, D.A. (2017). An Introduction to Modern Astrophysics, Second Edition (Cambridge University Press).

46. Scheiner, S. (2000). Calculation of isotope effects from first principles. Biochim. Biophys. Acta *1458*, 28–42. https://doi.org/10.1016/s0005-2728(00)00058-x.

47. Dartois, E. (2019). Interstellar carbon dust. C. *5*, 80. https://doi.org/10.3390/c5040080.

48. Rogantini, D., Costantini, E., Zeegers, S.T., Mehdipour, M., Psaradaki, I., Raassen, A.J.J., de Vries, C.P., and Waters, L.B.F.M. (2020). Magnesium and silicon in interstellar dust: X-ray overview. Astron. Astrophys. *641*, A149. https://doi.org/10.1051/0004-6361/201936805.

49. McClure, M.K., Rocha, W.R.M., Pontoppidan, K.M., Crouzet, N., Chu, L.E.U., Dartois, E., Lamberts, T., Noble, J.A., Pendleton, Y.J., Perotti, G., et al. (2023). An ice age JWST inventory of dense molecular cloud ices. Nat. Astron. *7*, 431–443. https://doi.org/10.1038/s41550-022-01875-w.

50. Herbst, E., and van Dishoeck, E.F. (2009). Complex organic interstellar molecules. Annu. Rev. Astron. Astrophys. *47*, 427–480. https://doi.org/10.1146/annurev-astro-082708-101654.

51. Hama, T., and Watanabe, N. (2013). Surface processes on interstellar amorphous solid water: adsorption, diffusion, tunneling reactions, and nuclear-spin conversion. Chem. Rev. *113*, 8783–8839. https://doi.org/10.1021/cr4000978.

52. Bergin, E.A., and Tafalla, M. (2007). Cold dark clouds: the initial conditions for star formation. Annu. Rev. Astron. Astrophys. *45*, 339–396. https://doi.org/10.1146/annurev.astro.45.071206.100404.

53. Prasad, S.S., and Tarafdar, S.P. (1983). UV radiation field inside dense clouds - its possible existence and chemical implications. Astrophys. J. *267*, 603–609. https://doi.org/10.1086/160896.

54. Yeghikyan, A.G. (2011). Irradiation of dust in molecular clouds. II. Doses produced by cosmic rays. Astrophysics *54*, 87–99. https://doi.org/10.1007/s10511-011-9160-2.

55. Bennett, C.J., Jamieson, C.S., Osamura, Y., and Kaiser, R.I. (2005). A combined experimental and computational investigation on the synthesis of acetaldehyde [CH_3CHO (X_1A')] in interstellar ices. Astrophys. J. *624*, 1097–1115. https://doi.org/10.1086/429119.

56. Bennett, C.J., Osamura, Y., Lebar, M.D., and Kaiser, R.I. (2005). Laboratory studies on the formation of three C_2H_4O isomers—acetaldehyde (CH_3CHO), ethylene oxide (c-C_2H_4O), and vinyl alcohol (CH_2CHOH)—in interstellar and cometary ices. Astrophys. J. *634*, 698–711. https://doi.org/10.1086/452618.

57. Abplanalp, M.J., Gozem, S., Krylov, A.I., Shingledecker, C.N., Herbst, E., and Kaiser, R.I. (2016). A study of interstellar aldehydes and enols as tracers of a cosmic ray-driven nonequilibrium synthesis of complex organic molecules. Proc. Natl. Acad. Sci. USA *113*, 7727–7732. https://doi.org/10.1073/pnas.1604426113.

58. Kleimeier, N.F., Turner, A.M., Fortenberry, R.C., and Kaiser, R.I. (2020). On the formation of the popcorn flavorant 2,3-butanedione ($CH_3COCOCH_3$) in acetaldehyde-containing interstellar ices. ChemPhysChem *21*, 1531–1540. https://doi.org/10.1002/cphc.202000116.

59. Kim, Y.S., and Kaiser, R.I. (2010). Abiotic formation of carboxylic acids (RCOOH) in interstellar and solar system model ices. Astrophys. J. *725*, 1002–1010. https://doi.org/10.1088/0004-637x/725/1/1002.

60. Zhu, C., Turner, A.M., Abplanalp, M.J., and Kaiser, R.I. (2018). Formation and high-order carboxylic acids (RCOOH) in interstellar analogous ices of carbon dioxide (CO_2) and methane (CH_4). ApJS. *234*, 15. https://doi.org/10.3847/1538-4365/aa9f28.

61. Bennett, C.J., Hama, T., Kim, Y.S., Kawasaki, M., and Kaiser, R.I. (2011). Laboratory studies on the formation of formic acid (HCOOH) in interstellar and cometary ices. Astrophys. J. *727*, 27. https://doi.org/10.1088/0004-637x/727/1/27.

62. Bergantini, A., Zhu, C., and Kaiser, R.I. (2018). A photoionization reflectron time-of-flight mass spectrometric study on the formation of acetic acid (CH_3COOH) in interstellar analog ices. Astrophys. J. *862*, 140. https://doi.org/10.3847/1538-4357/aacf93.

63. D'Hendecourt, L.B., and Jourdain de Muizon, M. (1989). The discovery of interstellar carbon dioxide. Astron. Astrophys. *223*, L5–L8.

64. Cheung, A.C., Rank, D.M., Townes, C.H., Thornton, D.D., and Welch, W.J. (1968). Detection of NH_3 molecules in the interstellar medium by their microwave emission. Phys. Rev. Lett. *21*, 1701–1705. https://doi.org/10.1103/PhysRevLett.21.1701.

65. Turner, A.M., and Kaiser, R.I. (2020). Exploiting photoionization reflectron time-of-flight mass spectrometry to explore molecular mass growth processes to complex organic molecules in interstellar and solar system ice analogs. Acc. Chem. Res. *53*, 2791–2805. https://doi.org/10.1021/acs.accounts.0c00584.

66. Bouilloud, M., Fray, N., Bénilan, Y., Cottin, H., Gazeau, M.-C., and Jolly, A. (2015). Bibliographic review and new measurements of the infrared band strengths of pure molecules at 25 K: H_2O, CO_2, CO, CH_4, NH_3, CH_3OH, HCOOH and H_2CO. Mon. Not. R. Astron. Soc. *451*, 2145–2160. https://doi.org/10.1093/mnras/stv1021.

67. Kleimeier, N.F., Eckhardt, A.K., and Kaiser, R.I. (2020). A mechanistic study on the formation of acetic acid (CH_3COOH) in polar interstellar analog ices exploiting photoionization reflectron time-of-flight mass spectrometry. Astrophys. J. *901*, 84. https://doi.org/10.3847/1538-4357/abafa4.

68. Krishtalik, L.I. (2000). The mechanism of the proton transfer: an outline. Biochim. Biophys. Acta *1458*, 6–27. https://doi.org/10.1016/s0005-2728(00)00057-8.

69. Chen, C.-H. (2022). Deuterium Oxide and Deuteration in Biosciences (Springer).

70. Abplanalp, M.J., Borsuk, A., Jones, B.M., and Kaiser, R.I. (2015). On the formation and isomer specific detection of propenal (C_2H_3CHO) and cyclopropanone (c-C_3H_4O) in interstellar model ices—A combined FTIR and reflectron time-of-flight mass spectroscopic study. Astrophys. J. *814*, 45. https://doi.org/10.1088/0004-637x/814/1/45.

71. Abplanalp, M.J., Góbi, S., and Kaiser, R.I. (2019). On the formation and the isomer specific detection of methylacetylene (CH_3CCH), propene (CH_3CHCH_2), cyclopropane (c-C_3H_6), vinylacetylene (CH_2CHCCH), and 1,3-butadiene ($CH_2CHCHCH_2$) from interstellar methane ice analogues. Phys. Chem. Chem. Phys. *21*, 5378–5393. https://doi.org/10.1039/C8CP03921F.

72. Kostko, O., Bandyopadhyay, B., and Ahmed, M. (2016). Vacuum ultraviolet photoionization of complex chemical systems. Annu. Rev. Phys. Chem. *67*, 19–40. https://doi.org/10.1146/annurev-physchem-040215-112553.

73. Eckhardt, A.K., Bergantini, A., Singh, S.K., Schreiner, P.R., and Kaiser, R.I. (2019). Formation of glyoxylic acid in interstellar ices: A key entry point for prebiotic chemistry. Angew. Chem. Int. Ed. Engl. *58*, 5663–5667. https://doi.org/10.1002/anie.201901059.

74. Miessler, G., Fischer, P., and Tarr, D. (2013). Inorganic Chemistry, Fifth Edition (Pearson).

75. Bryantsev, V.S., Diallo, M.S., and Goddard, W.A., 3rd (2008). Calculation of solvation free energies of charged solutes using mixed cluster/continuum models. J. Phys. Chem. B *112*, 9709–9719. https://doi.org/10.1021/jp802665d.